

Efficient Soft-Input Soft-Output Detection of Dual-Layer MIMO Systems

Ahmad Gomaa and Louay M.A. Jalloul, *Senior Member, IEEE*

Abstract—A dual-layer multiple-input multiple-output (MIMO) system with multi-level modulation is considered. A computationally efficient soft-input soft-output receiver based on the *exact* max-log maximum a posteriori (max-log-MAP) principle is presented in the context of iterative detection and decoding. We show that the computational complexity of our exact max-log-MAP solution grows linearly with the constellation size and is also less than that of the best known methods of Turbo-LORD that only provide approximate solutions. Using decoder feedback to change the decision thresholds of the constellation symbols, we show that the exhaustive search operation boils down to a simple slicing operation.

I. INTRODUCTION

Iterative detection and decoding (IDD) techniques have been widely used [1]–[4] to improve the performance of multiple-input multiple-output (MIMO) systems. The detector utilizes the feedback from the decoder to enhance the accuracy of its output statistics. In [1], [2], the detector was designed as a linear minimum mean square error equalizer, accepting soft input from the channel decoder. The soft input was used to cancel the interference from other streams and to adapt the equalization (weight) vector by modifying the variance of the canceled streams. In [3], the detector was designed as a decision feedback equalizer with successive cancellation at the symbol level before passing the log-likelihood ratios (LLRs) of the code bits to the decoder. In [4], IDD was used to mitigate the effect of inter-cell interference in orthogonal frequency division multiplexing (OFDM) systems. In [5]–[7], a maximum a posteriori (MAP) approximating algorithm was proposed as an improvement over the layered orthogonal lattice detector (LORD) approach [8], [9]. In [10], list detectors were proposed in addition to iterative channel estimation in OFDM systems. Other MAP approximation algorithms were proposed in [11]–[14] where modified sphere detection techniques were used.

Dual-layer transmission schemes are widely used in current cellular systems where user equipments cannot easily support more than two antennas. The solution presented in this paper is an *exact* solution of the max-log MAP detector for dual-layer systems and uses fewer metric computations than the approximate solution provided in [5], [6]. To generate the LLRs for one layer, we use the a-priori LLRs generated by the turbo decoder for the other layer to modify its decision thresholds and then use the slicer as a simple search device.

The rest of the paper is organized as follows. The system model is described in Section II, and the exact max-log MAP solution is derived in Section III. In Section IV, we prove

that the a-priori probabilities can lead to constellation symbols with empty decision regions. In Section V, we provide the complete algorithm and describe it in pseudo code. We analyze the algorithm computational complexity and compare its complexity with other algorithms in Section VI, and the paper is concluded in Section VII.

Notations: Unless otherwise stated, lower case and upper case bold letters denote vectors and matrices, respectively, and \mathbf{I}_m denotes the identity matrix of size m . Furthermore, $|\cdot|$ and $\|\cdot\|$ denote the absolute value and the l_2 -norm, respectively, while $(\cdot)^H$ denotes the complex conjugate transpose operation.

II. SYSTEM MODEL

We consider dual-layer transmission schemes, where two layers (streams) are transmitted over $N_t \geq 2$ antennas using the precoding matrix \mathbf{W} of size $N_t \times 2$. The receiver detects the transmitted streams using $N_r \geq 2$ receive antennas. The input-output relation is given by

$$\mathbf{y} = \bar{\mathbf{H}}\mathbf{W}\mathbf{s} + \mathbf{n} \triangleq \mathbf{H}\mathbf{s} + \mathbf{n} = \mathbf{h}_1 s_1 + \mathbf{h}_2 s_2 + \mathbf{n} \quad (1)$$

where \mathbf{y} , \mathbf{s} , \mathbf{n} and $\bar{\mathbf{H}}$ denote the $N_r \times 1$ received signal, 2×1 transmitted symbols, $N_r \times 1$ background noise plus inter-cell interference, and $N_r \times N_t$ channel matrix, respectively. Furthermore, \mathbf{h}_i is the i -th column vector of the equivalent channel matrix $\mathbf{H} = \bar{\mathbf{H}}\mathbf{W}$, and s_i is the i -th transmitted symbol chosen from the M -QAM constellation χ . The i -th M -QAM symbol, s_i , represents $q = \log_2(M)$ code bits $\mathbf{c}_i = [c_{i1} \ c_{i2} \ \dots \ c_{iq}]$. The above model suits single-carrier systems over flat fading channels and OFDM systems over frequency-selective channels where the relation in (1) applies to every subcarrier. In IDD, the detector computes the LLRs of the code bits and passes them to the channel decoder, which computes the extrinsic LLRs and feeds them back to the detector. The detector uses the a priori LLRs computed by the decoder to generate more accurate LLRs for the channel decoder and so forth. Assuming known channel and zero-mean circularly symmetric complex Gaussian noise \mathbf{n} of covariance matrix $\mathbf{C}_{\mathbf{nn}} = \mathbf{Q}^{-1}$, we write the log MAP a posteriori detector LLR of the bit c_{1k} as follows:

$$L(c_{1k}) = \log \left(\frac{\sum_{\bar{s}_1 \in \chi_{k,1}} P_{\bar{s}_1} \sum_{\bar{s}_2 \in \chi} \exp(-\|\mathbf{y} - \mathbf{h}_1 \bar{s}_1 - \mathbf{h}_2 \bar{s}_2\|_{\mathbf{Q}}^2) P_{\bar{s}_2}}{\sum_{\bar{s}_1 \in \chi_{k,0}} P_{\bar{s}_1} \sum_{\bar{s}_2 \in \chi} \exp(-\|\mathbf{y} - \mathbf{h}_1 \bar{s}_1 - \mathbf{h}_2 \bar{s}_2\|_{\mathbf{Q}}^2) P_{\bar{s}_2}} \right) \quad (2)$$

where $\|\mathbf{x}\|_{\mathbf{Q}}^2 \triangleq \mathbf{x}^H \mathbf{Q} \mathbf{x}$, $\chi_{k,1}$ and $\chi_{k,0}$ denote the constellation sets where the k -th bit are '1' and '0', respectively, and $P_{\bar{s}_i}$

and $P_{\bar{s}_2}$ denote the a priori probabilities that $s_1 = \bar{s}_1$ and $s_2 = \bar{s}_2$, respectively. The max-log MAP approximation of the LLR of c_{1k} is given by:

$$\begin{aligned} L(c_{1k}) &= \max_{\bar{s}_1 \in \chi_{k,1}} \left(\log P_{\bar{s}_1} + \max_{\bar{s}_2 \in \chi} (\log P_{\bar{s}_2} - \|\mathbf{y} - \mathbf{h}_1 \bar{s}_1 - \mathbf{h}_2 \bar{s}_2\|_{\mathbf{Q}}^2) \right) \\ &\quad - \max_{\bar{s}_1 \in \chi_{k,0}} \left(\log P_{\bar{s}_1} + \max_{\bar{s}_2 \in \chi} (\log P_{\bar{s}_2} - \|\mathbf{y} - \mathbf{h}_1 \bar{s}_1 - \mathbf{h}_2 \bar{s}_2\|_{\mathbf{Q}}^2) \right) \end{aligned} \quad (3)$$

Similarly, the max-log MAP LLR of c_{2k} is:

$$\begin{aligned} L(c_{2k}) &= \max_{\bar{s}_2 \in \chi_{k,1}} \left(\log P_{\bar{s}_2} + \max_{\bar{s}_1 \in \chi} (\log P_{\bar{s}_1} - \|\mathbf{y} - \mathbf{h}_1 \bar{s}_1 - \mathbf{h}_2 \bar{s}_2\|_{\mathbf{Q}}^2) \right) \\ &\quad - \max_{\bar{s}_2 \in \chi_{k,0}} \left(\log P_{\bar{s}_2} + \max_{\bar{s}_1 \in \chi} (\log P_{\bar{s}_1} - \|\mathbf{y} - \mathbf{h}_1 \bar{s}_1 - \mathbf{h}_2 \bar{s}_2\|_{\mathbf{Q}}^2) \right) \end{aligned} \quad (4)$$

The brute force solution of (3) (and similarly (4)) requires the computation of M^2 metrics where, for each instance of \bar{s}_1 , the metric $(\log P_{\bar{s}_2} - \|\mathbf{y} - \mathbf{h}_1 \bar{s}_1 - \mathbf{h}_2 \bar{s}_2\|_{\mathbf{Q}}^2)$ is computed for all instances of \bar{s}_2 . However, we show in Section III how we obtain the *exact* max-log MAP solution for the LLRs using fewer than $4M$ (rather than M^2) metrics computations.

III. EXACT MAX-LOG MAP SOLUTION

The main strategy of our solution is to convert the l_2 -norms in (3) and (4) into simple absolute values fitted for the slicing operations. Then, we exploit the a-priori LLRs to control the thresholds of the slicers. We begin by whitening the noise to get $\tilde{\mathbf{y}} = \sqrt{\mathbf{Q}}\mathbf{y}$ and $\tilde{\mathbf{h}}_i = \sqrt{\mathbf{Q}}\mathbf{h}_i$. We then rewrite the bottleneck maximization problem $\max_{\bar{s}_2 \in \chi} (\log P_{\bar{s}_2} - \|\mathbf{y} - \mathbf{h}_1 \bar{s}_1 - \mathbf{h}_2 \bar{s}_2\|_{\mathbf{Q}}^2)$ as follows:

$$\begin{aligned} &\max_{\bar{s}_2 \in \chi} (\log P_{\bar{s}_2} - \|\tilde{\mathbf{y}} - \tilde{\mathbf{h}}_1 \bar{s}_1 - \tilde{\mathbf{h}}_2 \bar{s}_2\|^2) \\ &= \max_{\bar{s}_2 \in \chi} \left(\log P_{\bar{s}_2} - \|\tilde{\mathbf{h}}_2\|^2 \left\| \frac{(\tilde{\mathbf{y}} - \tilde{\mathbf{h}}_1 \bar{s}_1)}{\|\tilde{\mathbf{h}}_2\|} - \mathbf{B} \begin{bmatrix} \bar{s}_2 \\ \mathbf{0} \end{bmatrix} \right\|^2 \right) \end{aligned} \quad (5)$$

where $\mathbf{0}$ is all-zero vector of length $N_r - 1$, $\mathbf{B} = \begin{bmatrix} \tilde{\mathbf{h}}_2 & \mathbf{E} \end{bmatrix}$ is an $N_r \times N_r$ unitary matrix as \mathbf{E} is an $N_r \times (N_r - 1)$ matrix chosen such that $\mathbf{E}^H \tilde{\mathbf{h}}_2 = \mathbf{0}$ and $\mathbf{E}^H \mathbf{E} = \mathbf{I}$. The reason we write the matrix \mathbf{B} in this form is to exploit its unitary structure and take it as a common factor out of the norm without affecting its value. This will lead to converting the l_2 -norm into a single absolute value as follows. Since $\mathbf{B}^H \mathbf{B} = \mathbf{I}_2$, we rewrite the maximization as follows:

$$\begin{aligned} &\max_{\bar{s}_2 \in \chi} \left(\log P_{\bar{s}_2} - \|\tilde{\mathbf{h}}_2\|^2 \left\| \frac{\mathbf{B}^H (\tilde{\mathbf{y}} - \tilde{\mathbf{h}}_1 \bar{s}_1)}{\|\tilde{\mathbf{h}}_2\|} - \begin{bmatrix} \bar{s}_2 \\ \mathbf{0} \end{bmatrix} \right\|^2 \right) \\ &= \max_{\bar{s}_2 \in \chi} \left(\frac{\log P_{\bar{s}_2}}{\|\tilde{\mathbf{h}}_2\|^2} - |Z_{(\bar{s}_1)} - \bar{s}_2|^2 \right) \end{aligned} \quad (6)$$

where $Z_{(\bar{s}_1)} = \tilde{\mathbf{h}}_2^H (\tilde{\mathbf{y}} - \tilde{\mathbf{h}}_1 \bar{s}_1) / \|\tilde{\mathbf{h}}_2\|^2$. If the a-priori probability term $(\log P_{\bar{s}_2} / \|\tilde{\mathbf{h}}_2\|^2)$ were not there [15] (i.e., ML instead of MAP), then the solution of the maximization in (6) would be a simple slicer, and only $2M$ metrics (enumeration

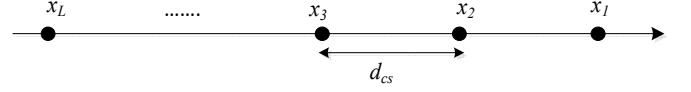


Fig. 1. L -PAM constellation for the real (or imaginary) part of the M -QAM constellation.

over \bar{s}_1 and \bar{s}_2 in (3) and (4)) were to be computed to obtain the LLRs of the code bits corresponding to s_1 and s_2 . With the a-priori probability term, we obtain the *exact* solution of (6) with a reasonable increase in the number of metrics computations which is, interestingly, less than that of the approximate solution in [5], [6]. In modern communications standards [16], the real and imaginary parts of \bar{s}_2 correspond to two orthogonal L -PAM constellations, ψ , where $L = \sqrt{M}^1$. In Fig. 1, we show the L -PAM one-dimensional constellation corresponding to the real or imaginary of any complex QAM constellation. Hence, we rewrite (6) as follows:

$$\begin{aligned} &\max_{\bar{s}_2 \in \chi} \left(\frac{\log P_{\bar{s}_2}}{\|\tilde{\mathbf{h}}_2\|^2} - |Z_{(\bar{s}_1)} - \bar{s}_2|^2 \right) \\ &= \max_{\bar{s}_{2,r} \in \psi} \left(\frac{\log P_{\bar{s}_{2,r}}}{\|\tilde{\mathbf{h}}_2\|^2} - |Z_{\bar{s}_{1,r}} - \bar{s}_{2,r}|^2 \right) \\ &\quad + \max_{\bar{s}_{2,I} \in \psi} \left(\frac{\log P_{\bar{s}_{2,I}}}{\|\tilde{\mathbf{h}}_2\|^2} - |Z_{\bar{s}_{1,I}} - \bar{s}_{2,I}|^2 \right) \end{aligned} \quad (7)$$

where $Z_{\bar{s}_{1,r}}$ and $Z_{\bar{s}_{1,I}}$ denote the real and imaginary parts of $Z_{(\bar{s}_1)}$, respectively. Furthermore, $P_{\bar{s}_{2,r}}$ and $P_{\bar{s}_{2,I}}$ denote the a-priori probabilities that the real and imaginary parts of s_2 equal $\bar{s}_{2,r}$ and $\bar{s}_{2,I}$, computed using the a-priori LLRs of the bits corresponding to the real and imaginary parts, respectively.

Next, we use the a-priori probabilities (LLRs) to modify the decision regions of the L -PAM real and imaginary symbols; correspondingly apply the slicer to the real and imaginary parts of $Z_{(\bar{s}_1)} = \tilde{\mathbf{h}}_2^H (\tilde{\mathbf{y}} - \tilde{\mathbf{h}}_1 \bar{s}_1) / \|\tilde{\mathbf{h}}_2\|^2$, respectively, to find the solution of (7); and then compute the metrics in (3) and (4), which can be significantly simplified using (7). To develop the method of modifying the decision boundaries, we derive the decision region of the symbol x_1 in Fig. 1 by writing the conditions on $Z_{\bar{s}_{1,r}}$ such that

$$\frac{\log P_{x_1}}{\|\tilde{\mathbf{h}}_2\|^2} - |Z_{\bar{s}_{1,r}} - x_1|^2 > \frac{\log P_{x_j}}{\|\tilde{\mathbf{h}}_2\|^2} - |Z_{\bar{s}_{1,r}} - x_j|^2, \forall j \neq 1 \quad (8)$$

Simplifying (8), we get the decision region of x_1 as follows:

$$Z_{\bar{s}_{1,r}} > \max_{j>1} \left(\frac{x_1 + x_j}{2} - \frac{\log(P_{x_1}/P_{x_j})}{2(x_1 - x_j)\|\tilde{\mathbf{h}}_2\|^2} \right) \quad (9)$$

Similarly, the decision region of x_k is given by

$$\max_{j>k} D_{kj} < Z_{\bar{s}_{1,r}} < \min_{j<k} D_{kj}, \quad 1 < k < L \quad (10)$$

and the decision region of the last symbol x_L is given by

$$Z_{\bar{s}_{1,r}} < \min_{j<L} D_{Lj} \quad (11)$$

$$\text{where } D_{kj} = D_{jk} = \frac{x_k + x_j}{2} - \frac{\log(P_{x_k}/P_{x_j})}{2(x_k - x_j)\|\tilde{\mathbf{h}}_2\|^2} \quad (12)$$

¹Assuming square constellation, without loss of generality.

is called the *probabilistic boundary* between the constellation symbols x_j and x_k . Equation (12) shows that the boundary between two neighboring symbols moves towards the symbol with the lower a-priori probability, tending to shrink its decision region while extending that of the symbol with the higher a-priori probability. Equation (12) also shows that without a-priori LLRs (i.e., $P_{x_k} = \frac{1}{L}$, $\forall k$), the boundaries between symbols return to their original values (the average of constellation symbols amplitudes).

IV. SYMBOLS WITH EMPTY DECISION REGIONS

We prove that the a-priori probability distribution can lead to constellation symbols with empty decision regions that will not be chosen by the slicer regardless of $Z_{\bar{s}_1, r}$ (or $Z_{\bar{s}_1, I}$).

Theorem 1: When computing the lower bound of the decision region for the constellation symbol x_k , given by $\max_{j>k} D_{kj}$, the following can occur:

$$j^* > k + 1, \quad \text{where} \quad j^* \equiv \arg \max_{j>k} D_{kj} \quad (13)$$

meaning that the lower bound of the symbol x_k is not determined by its boundary with the adjacent symbol x_{k+1} , but determined instead by its boundary with a farther symbol $x_{j^*} < x_{k+1}$. In this case, all symbols lying between x_k and x_{j^*} (i.e., the constellation symbols x_m , where $k < m < j^*$) do not have decision regions and will not be chosen regardless of the decision statistic value.

Proof: From (10), the decision boundaries for x_m , where $k < m < j^*$, are given by

$$\begin{aligned} \max(D_{m(m+1)}, \dots, D_{mj^*}, \dots, D_{mL}) &< Z_{\bar{s}_1, r} \\ &< \min(D_{m(m-1)}, \dots, D_{mk}, \dots, D_{m1}) \end{aligned} \quad (14)$$

However, there is no value for $Z_{\bar{s}_1, r}$ that satisfies (14) if

$$D_{mk} < D_{mj^*} \quad (15)$$

In the sequel, we prove that the condition in (15) is satisfied if $j^* = \arg \max_{j>k} D_{kj}$, i.e., $D_{kj^*} > D_{km}$ and, hence,

$$x_{j^*} - x_m > \frac{\log(P_{x_k}/P_{x_{j^*}})}{2(x_k - x_{j^*})\|\tilde{\mathbf{h}}_2\|^2} - \frac{\log(P_{x_k}/P_{x_m})}{2(x_k - x_m)\|\tilde{\mathbf{h}}_2\|^2} \quad (16)$$

$$(m - j^*)d_{cs} > \frac{\log\left((P_{x_k}/P_{x_{j^*}})^{m-k} (P_{x_m}/P_{x_k})^{j^*-k}\right)}{(j^* - k)(m - k)d_{cs}\|\tilde{\mathbf{h}}_2\|^2} \quad (17)$$

where $x_k - x_{j^*} = (j^* - k)d_{cs}$ and d_{cs} is the separation between adjacent real (or imaginary) constellation symbols as shown in Fig. 1. Since $k < m < j^*$, we define

$$m = k + f, \quad j^* = m + g = k + f + g \quad (18)$$

where $f, g \in \{0, \mathbb{Z}^+\}$. We rewrite (17) as follows:

$$fg(f+g)d_{cs}^2\|\tilde{\mathbf{h}}_2\|^2 < \log\left((P_{x_{j^*}}/P_{x_m})^f (P_{x_k}/P_{x_m})^g\right) \quad (19)$$

Next, we rewrite the condition in (15) as follows:

$$D_{mk} - D_{mj^*} = \frac{(f+g)d_{cs}}{2} - \frac{\log\left(\left(\frac{P_{x_k}}{P_{x_m}}\right)^g \left(\frac{P_{x_{j^*}}}{P_{x_m}}\right)^f\right)}{2fgd_{cs}\|\tilde{\mathbf{h}}_2\|^2} \quad (20)$$

Using the inequality in (19), we bound $D_{mk} - D_{mj^*}$ as follows:

$$\begin{aligned} D_{mk} - D_{mj^*} &< \frac{(f+g)d_{cs}}{2} - \frac{fg(f+g)d_{cs}^2\|\tilde{\mathbf{h}}_2\|^2}{2fgd_{cs}\|\tilde{\mathbf{h}}_2\|^2} \\ D_{mk} - D_{mj^*} &< 0, \quad D_{mk} < D_{mj^*} \end{aligned} \quad (21)$$

which concludes the proof. \blacksquare

The practical importance of this theorem is that it can reduce the algorithm complexity and further speed it up. For example, if the lower boundary of x_1 is determined by x_4 then we do not need to compute the decision boundaries of x_2 and x_3 because they will have empty decision regions.

V. ALGORITHM AND COMPUTATIONAL COMPLEXITY

In the sequel, we summarize the algorithm and show the receiver model in Fig. 2.

Preprocessing: Compute $\mathbf{H} = \bar{\mathbf{H}}\mathbf{W}$ and whiten the noise by computing $\tilde{\mathbf{y}} = \sqrt{\mathbf{Q}}\mathbf{y}$, $\tilde{\mathbf{h}}_1 = \sqrt{\mathbf{Q}}\mathbf{h}_1$, and $\tilde{\mathbf{h}}_2 = \sqrt{\mathbf{Q}}\mathbf{h}_2$.

Procedure:

- 1) Get the decision regions for $Z_{\bar{s}_1, r}$, $Z_{\bar{s}_1, I}$, $Z_{\bar{s}_2, r}$, and $Z_{\bar{s}_2, I}$ using the corresponding a priori LLRs as follows: Initialize $k = 1$.

While $k \leq L$

A) Compute the lower and upper thresholds of the k -th constellation symbol as $\max_{j>k} D_{kj}$ and $\min_{j<k} D_{kj}$, respectively, where

$$D_{kj} = \frac{x_k + x_j}{2} - \frac{\sum_{n=1}^{q/2} ((b_{n,k} - b_{n,j})L_a(c_{in}))}{2(x_k - x_j)\|\tilde{\mathbf{h}}_i\|^2} \quad (22)$$

where $i \in \{1, 2\}$, $L_a(c_{in})$ denotes the a priori LLR of the code bit c_{in} , and $\{b_{n,k}, b_{n,j}\}_{n=1}^{q/2} \in \{0, 1\}$ are the bit vectors corresponding to the constellation symbols x_k and x_j , respectively. The transition from the probability domain in (12) to the LLR domain in (22) is straightforward.

B) **If** $j^* > k + 1$, where $j^* \equiv \arg \max_{j>k} D_{kj}$, set the decision regions of the symbols x_m , where $k < m < j^*$, to empty, and set $k = j^*$.

Else, set $k = k + 1$.

End While

- 2) Enumeration step over constellation points of s_1 and s_2 .

For $k = 1 : M$

a) Compute the following quantities for $\bar{s}_1(k)$, $\bar{s}_2(k) \in \chi$

$$Z_{(\bar{s}_1)} = \frac{\tilde{\mathbf{h}}_2^H}{\|\tilde{\mathbf{h}}_2\|^2} (\tilde{\mathbf{y}} - \tilde{\mathbf{h}}_1 \bar{s}_1(k)), \quad Z_{(\bar{s}_2)} = \frac{\tilde{\mathbf{h}}_1^H}{\|\tilde{\mathbf{h}}_1\|^2} (\tilde{\mathbf{y}} - \tilde{\mathbf{h}}_2 \bar{s}_2(k))$$

b) Slice the real and imaginary parts of $Z_{(\bar{s}_1)}$ and $Z_{(\bar{s}_2)}$ using the thresholds obtained in Step 1 to obtain $\bar{s}_2^*(k)$ and $\bar{s}_1^*(k)$, respectively.

c) Compute the following metrics

$$\begin{aligned} \eta_1(k) &= \sum_{n=1}^q (\bar{b}_{1,n}(k)L_a(c_{1n}) + \bar{b}_{2,n}^*(k)L_a(c_{2n})) \\ &\quad - \|\tilde{\mathbf{y}} - \tilde{\mathbf{h}}_1 \bar{s}_1(k) - \tilde{\mathbf{h}}_2 \bar{s}_2^*(k)\|^2 \end{aligned} \quad (23)$$

$$\begin{aligned} \eta_2(k) &= \sum_{n=1}^q (\bar{b}_{1,n}^*(k)L_a(c_{1n}) + \bar{b}_{2,n}(k)L_a(c_{2n})) \\ &\quad - \|\tilde{\mathbf{y}} - \tilde{\mathbf{h}}_1 \bar{s}_1^*(k) - \tilde{\mathbf{h}}_2 \bar{s}_2(k)\|^2 \end{aligned} \quad (24)$$

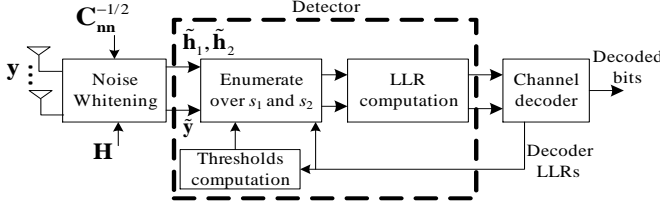


Fig. 2. Receiver model with our proposed approach.

where $\{\bar{b}_{1,n}(k), \bar{b}_{2,n}(k), \bar{b}_{1,n}^*(k), \bar{b}_{2,n}^*(k)\}_{n=1}^q$ are the bit vectors of $\bar{s}_1(k), \bar{s}_2(k), \bar{s}_1^*(k), \bar{s}_2^*(k)$, respectively.

End For

3) Compute the detector LLRs for $i = 1, 2$ and $0 \leq n \leq q$

$$L(c_{in}) = \max_{k: \bar{b}_{i,n}(k)=1} \eta_i(k) - \max_{k: \bar{b}_{i,n}(k)=0} \eta_i(k) \quad (25)$$

VI. COMPLEXITY ANALYSIS

We count the number of required metrics computations to obtain the $2\log_2(M)$ detector LLRs corresponding to s_1 and s_2 . To get the new decision regions, we need to compute the probabilistic boundaries between every two symbols of the L symbols (for both real and imaginary parts). Since $D_{jk} = D_{kj}$, the number of metrics (boundaries) to be computed is

$$N_{metrics}^{s_1} = 2 \frac{L(L-1)}{2} = L^2 - L = M - \sqrt{M} < M \quad (26)$$

Note that these boundaries are computed only once and are not included inside the enumeration over s_1 in (3). Hence, the total number of metric computations to obtain the LLRs of the code bits corresponding to s_1 is $M + N_{metrics}^{s_1} = 2M - \sqrt{M}$. To obtain the $2q$ LLRs corresponding to s (i.e., s_1 and s_2), the number of metric computations per tone becomes

$$N_{metrics}^{Total} = 4M - 2\sqrt{M} < 4M \quad (27)$$

In Table I, we compare our algorithm with the Turbo-LORD (T-LORD) [5] and the brute-force algorithms in terms of the number of metrics to be computed, number of real multiplications (Muls), and number of real additions (Adds) per tone per iteration as function of the constellation size and the number of receive antennas. In Table II, we compare these algorithms for 256-QAM and two receive antennas where we observe the significant computational complexity saving without any performance loss since our algorithm obtains the exact solution rather than the approximate solution in [5]. In T-LORD [5], while enumerating over s_1 , three candidates for s_2 are obtained for every possible value of the M candidates of s_1 . Hence, we have $3M$ candidates for the (s_1, s_2) pair, and the metric in (23) is computed for each candidate. Doing the same for s_2 , we have another $3M$ metrics summing up to $6M$ metrics to be computed.

VII. CONCLUSION

We developed the *exact* max-log MAP detector for IDD in dual-layer MIMO schemes with computational complexity less than $4M$. The idea is to use the a priori LLRs in modifying the decision thresholds of the constellation symbols. We also showed that the a priori LLRs can lead to constellation

TABLE I
COMPLEXITY COMPARISON BETWEEN VARIOUS ML DETECTORS

Detector	Metrics	Real Muls	Real Adds
Proposed	$4M - 2\sqrt{M}$	$(16N_r + 18)M - 2\sqrt{M}$	$(12N_r + 3q + 18)M - (q + 2)\sqrt{M} - 4$
T-LORD	$6M$	$(16N_r + 48)M$	$(12N_r + 2q + 52)M - 4$
Brute force	M^2	$8M^2$	$12M^2 - 4M$

TABLE II
COMPLEXITY OF VARIOUS ML DETECTORS FOR $M = 256$ AND $N_r = 2$

Detector	Metrics	Real Muls	Real Adds
Proposed	992	12768	16732
T-LORD	1536	20480	23548
Brute force	65536	524288	785408

symbols with empty decision regions, reducing the search space of the slicing block. Comparing the computational complexity with the Turbo-LORD approximate solution and the exact brute force solutions, we show that our algorithm achieves significant complexity reduction while achieving the exact max-log MAP solution. We have numerically verified that our method yields the same performance as the brute force solution for various simulation parameters but the simulation results are not shown here due to space limitations.

REFERENCES

- [1] M. Tuchler, A. Singer, and R. Koetter, "Minimum mean squared error equalization using a priori information," *IEEE Transactions on Signal Processing*, vol. 50, no. 3, pp. 673–683, 2002.
- [2] M. Sellathurai and S. Haykin, "Turbo-BLAST for wireless communications: theory and experiments," *IEEE Transactions on Signal Processing*, vol. 50, no. 10, pp. 2538–2546, 2002.
- [3] J. Choi, A. Singer, L. Jungwoo, and N. Cho, "Improved linear soft-input soft-output detection via soft feedback successive interference cancellation," *IEEE Trans. on Comm.*, vol. 58, no. 3, pp. 986–996, 2010.
- [4] M. Mikami and T. Fujii, "Iterative MIMO signal detection with inter-cell interference cancellation for downlink transmission in coded OFDM cellular systems," in *IEEE Vehicular Technology Conference*, 2009.
- [5] A. Tomasoni, M. Sitti, M. Ferrari, and S. Bellini, "Low complexity, quasi-optimal MIMO detectors for iterative receivers," *IEEE Transactions on Wireless Communications*, vol. 9, no. 10, pp. 3166–3177, 2010.
- [6] —, "Turbo-LORD: A MAP-approaching soft-input soft-output detector for iterative MIMO receivers," in *IEEE Global Telecomm. Conference*, 2007, pp. 3504–3508.
- [7] —, "A K-best version of the turbo-LORD MIMO detector in realistic settings," in *IEEE International Conference on Communications*, 2009.
- [8] M. Sitti and M. Fitz, "Layered orthogonal lattice detector for two transmit antenna communications," in *Allerton Conference On Communication, Control, And Computing*, 2005.
- [9] —, "A novel soft-output layered orthogonal lattice detector for multiple antenna communications," in *IEEE ICC*, 2006.
- [10] J. Ylioinas and M. Juntti, "Iterative joint detection, decoding, and channel estimation in turbo-coded MIMO-OFDM," *IEEE Transactions on Vehicular Technology*, vol. 58, no. 4, pp. 1784–1796, 2009.
- [11] J. Choi, Y. Hong, and J. Yuan, "An approximate MAP-based iterative receiver for MIMO channels using modified sphere detection," *IEEE Trans. on Wireless Communications*, vol. 5, no. 8, pp. 2119–2126, 2006.
- [12] H. Vikalo, B. Hassibi, and T. Kailath, "Iterative decoding for MIMO channels via modified sphere decoding," *IEEE Transactions on Wireless Communications*, vol. 3, no. 6, pp. 2299–2311, 2004.
- [13] S. Han, T. Cui, and C. Tellambura, "Improved K-best sphere detection for uncoded and coded MIMO systems," *IEEE Wireless Communications Letters*, vol. 1, no. 5, pp. 472–475, 2012.
- [14] B. Hochwald and T. Brink, "Achieving near-capacity on a multiple-antenna channel," *IEEE Transactions on Communications*, vol. 51, no. 3, pp. 389–399, 2003.
- [15] R. Ghaffar and R. Knopp, "Interference sensitivity for multiuser MIMO in LTE," in *IEEE SPAWC Workshop*, 2011.
- [16] "Physical channels and modulation," *3GPP TS 36.211*, 2010–2013.